

Draw-ratio-dependent morphology of biaxially oriented polypropylene films as determined by atomic force microscopy

H.-Y. Nie*, M.J. Walzak, N.S. McIntyre

Surface Science Western, The University of Western Ontario, London, Ontario, Canada N6A 5B7

Received 8 February 1999; received in revised form 1 June 1999; accepted 1 June 1999

Abstract

Using atomic force microscopy we have examined the surface morphology of sequentially biaxially oriented polypropylene (BOPP) films. The surface was shown to be dominated by a nanometer-scale fiber-like network structure, the configuration of which was found to be determined by the relationship between the draw ratios used in the bi-directional stretching processes [machine draw (MD) and transverse draw (TD)]. For the film fabricated with MD and TD ratios of 5.2:1 and 9:1, respectively, preferential orientation of fine fibers to the TD direction and larger veins to the MD direction were observed. When MD and TD ratios became similar, no predominant TD direction fiber alignment and no larger veins were observed. We have shown that the residual effects of the first stretching of the film surface can provide information on the way in which morphological development of the BOPP occurs. © 1999 Elsevier Science Ltd. All rights reserved.

Keywords: Biaxially oriented polypropylene; Machine-draw and transverse-draw ratios; Atomic force microscopy

1. Introduction

The use of polypropylene (PP) in printing and adhesion applications requires surface modification in order to improve its adhesive properties [1]. Using atomic force microscopy (AFM) [2], we had previously investigated the surface modification of a biaxially oriented PP (BOPP) film surface by UV–ozone treatment [3]. The modified surface in this instance showed an improvement of adhesion and the formation of low-molecular-weight-oxidized materials into mounds [3]. Although the study of the modified surface is very important in understanding the effects of the treatment, study of the microscopic surface structure of the untreated PP film is also important to understand the morphology formation of polymer films made by stretching.

There have been reports of spherulitic structures on PP studied with scanning electron microscopy [4] and transmission electron microscopy [5,6] and, more recently, AFM has also been used to measure the surface morphology of PP. Most of the AFM work has concentrated on obtaining atomic resolution for the examination of crystalline PP [6–8]. There are reports of nanometer-scale fiber formation on shear-deformed isotactic [9] and hard elastic [10] PP surfaces. There is also an AFM study of corona-treated

BOPP film, emphasizing the formation of mounds caused the treatment [11].

In this paper, we examine morphological development of BOPP films dependent on the relationship between the bi-directional stretching ratios. We will show that the surface of the BOPP films is characterized by a nanometer-scale fiber-like network structure. For a film fabricated with greater difference between the bi-directional stretching ratios, additional vein structures were also found superimposed on the fine network. These vein structures provide information on the effects of the initial stretching which remains even after the subsequent stretching in the perpendicular direction during the biaxial-orientation process. We will also show that lateral force imaging, using contact mode AFM, is useful for delineation of the vein structures through enhancement of the edges of topographic features. When bi-directional stretching ratios become similar, there is no vein structure and network structure on the surface is much more homogeneous. We used two such BOPP films fabricated using different draw ratios and confirmed that the morphology, as well as the formation of veins, is determined by the relationship between the bi-directional draw ratios.

2. Experimental

Both contact and non-contact modes of a commercial AFM (Explorer, TopoMetrix) were used in this study. In

*Corresponding author. Tel: +1-519-661-2173; fax: +1-519-661-3709.
E-mail address: hynie@surf.ssw.uwo.ca (H.-Y. Nie)

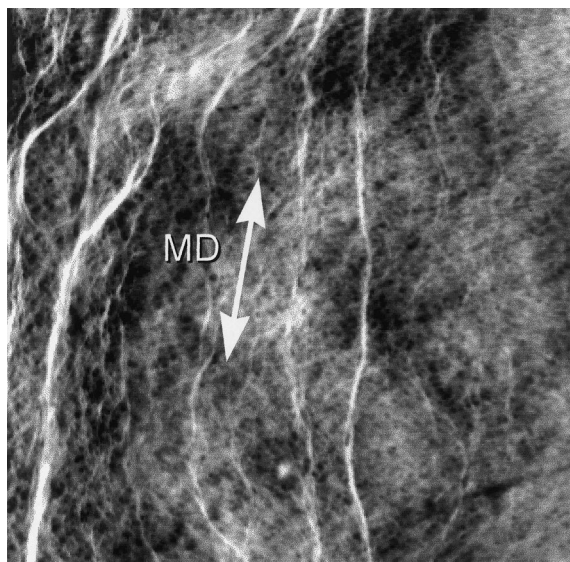


Fig. 1. A non-contact mode AFM topographic image (scan area: $20 \times 20 \mu\text{m}^2$) obtained from BOPP-1 (MD and TD ratios are 5.2:1 and 9:1, respectively). The insert arrow shows the MD direction (TD direction is perpendicular to the MD direction). The gray-scale range for the image is 76 nm.

contact mode, a soft cantilever with a sharp tip on its free end was used to probe the interaction between the tip and sample surface. The V-shaped silicon nitride cantilever had a nominal spring constant of 0.03 N/m. The cantilever was $0.6 \mu\text{m}$ thick, $18 \mu\text{m}$ wide and $200 \mu\text{m}$ long with a “super tip” attached whose apex radius was about 20 nm, which was measured using scanning electron microscopy. In contact mode, the tip is in contact with the surface so that both the deflection and torsion of the cantilever can be determined by measuring the position of the reflection of

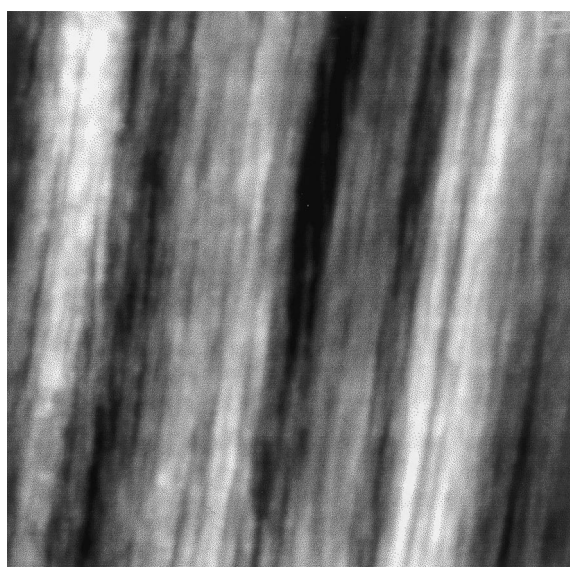


Fig. 2. A non-contact mode AFM topographic image (scan area: $2.5 \times 2.5 \mu\text{m}^2$) for a uniaxially oriented (only in the MD direction as shown by the arrow in Fig. 1) PP film. The gray-scale range is 24 nm.

a laser light on a four-segment photodetector. The laser light is directed onto the back of the cantilever and the position of the reflection changes with changes in the cantilever position. The applied force between the tip and surface is kept constant (repulsive force of 1–5 nN was used in this study) by adjusting the sample height when scanning, and in this way, surface features are imaged. During forward or reverse (bi-directional) scanning of the tip across the surface, the torsion on the cantilever due to the interaction between the tip and surface can be used to detect different lateral forces [12] which are used to construct the lateral force image. The direct output of the photodetector corresponding to the torsional movement of the cantilever, in units of nA, is the photo-induced current used to construct the lateral force image.

In non-contact mode, a stiff silicon cantilever (spring constant: $\sim 30 \text{ N/m}$), $130 \mu\text{m}$ long, $29 \mu\text{m}$ wide and $3.7 \mu\text{m}$ thick, was used. The tip apex radius was $\sim 20 \text{ nm}$ as estimated from scanning electron microscopy measurement. The cantilever was oscillated at its resonant frequency ($\sim 280 \text{ kHz}$). The amplitude of the oscillation decreases when the tip is brought close enough to the surface so that the tip “feels” the attractive and repulsive forces. Non-contact mode AFM functions by keeping a damped constant oscillation amplitude as the tip scans over the surface. In the present study, the cantilever was oscillated at high amplitudes and the set point for imaging was 50%, i.e. the amplitude was damped to half of its amplitude in free space due to the interaction between the tip and surface.

Thermally extruded, biaxially oriented isotactic polypropylene film (3M Company) was used in this study. The 0.03-mm thick BOPP film was produced from a homopolymer resin ($M_w = 1.9 \times 10^5$, polydispersity = 6.0). The base resin contains 500–1000 ppm each of an inorganic acid scavenger and a high-molecular-weight phenolic antioxidant. The PP was produced on a tenter frame film line and quenched at 45°C prior to orientation. The BOPP film was formed with machine-draw (MD) and transverse-draw (TD) ratios of 5.2:1 and 9:1, respectively (BOPP-1). A second BOPP film (BOPP-2), fabricated with MD and TD ratios of 8:1 and 8.7:1, respectively, was used to investigate the change in morphology with the change in relationship between the two draw ratios. A uniaxially oriented PP film (i.e. before the TD) was also used to examine the bi-directional stretching effect.

All images were obtained in air with a typical humidity of about 50%. Each image consisted of 500 lines with 500 pixel points per line. Images of areas of 20 and $2.5 \mu\text{m}^2$ were obtained with scan rates of 100 and $20 \mu\text{m/s}$, respectively. We confirmed that no apparent differences in images were caused when the above scan rates were decreased to 50 and $10 \mu\text{m/s}$, respectively.

3. Results and discussion

Fig. 1 shows a non-contact mode AFM topographic

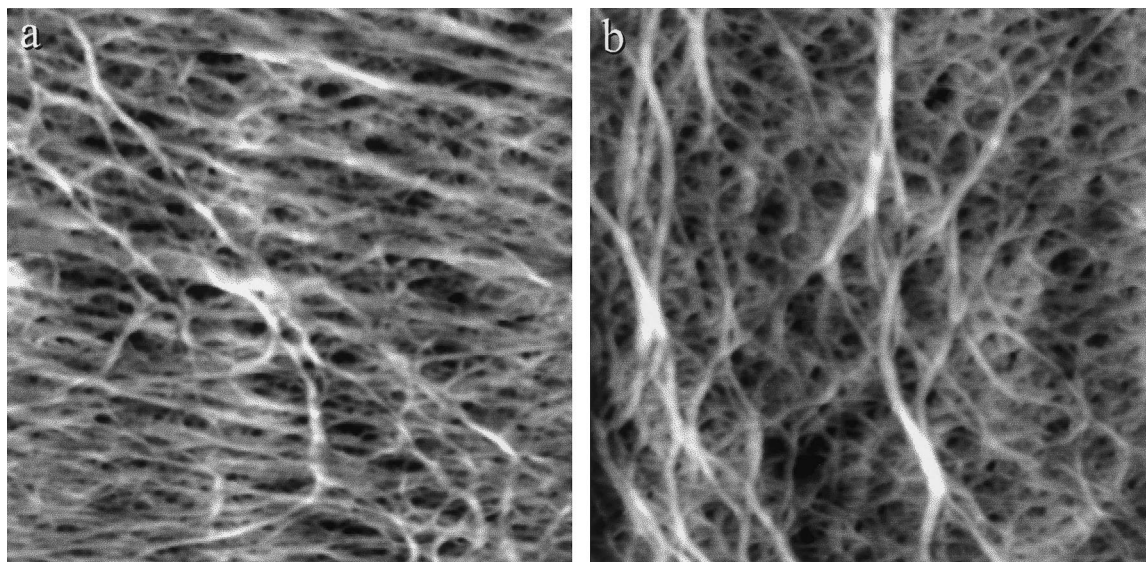


Fig. 3. Shown in (a) and (b) are two representative non-contact mode AFM topographic images (scan area: $2.5 \times 2.5 \mu\text{m}^2$) obtained on a part of the fiber-like network structure (“normal” surface) of the BOPP-1 film shown in Fig. 1. The MD direction is indicated by the arrow in Fig. 1. Gray-scale ranges for the topographic images in (a) and (b) are 20 and 33 nm, respectively.

image of an area $20 \mu\text{m}$ square obtained on the BOPP-1 film. The arrow insert in Fig. 1 shows the MD direction for this image and nominally for all other images presented in this paper. The TD direction is perpendicular to this MD direction. From the topographic image we can see a number of veins running nominally parallel to the MD direction. The surface morphology seen in the figure consists of two structures, the vein structure and the surface without the vein structure called hereafter the “normal” surface. The scan area was too large for the “normal” surface features to be revealed in this image. In order to clarify the detailed surface morphology of the BOPP-1 film and to explore its

formation mechanism, higher resolution images were obtained.

For a better understanding of the BOPP-1 film surface morphology development, we first show the morphology of a uniaxially oriented PP film, i.e. stretched only in the MD direction. Shown in Fig. 2 is a non-contact mode AFM topographic image of an area $2.5 \mu\text{m}$ square obtained on the uniaxially oriented PP film. From the image it is clear that strands are formed and are aligned parallel to the MD, the stretching direction. Although we did not have molecular resolution images on such polymer strands, we speculate that the isotactic PP molecular chains align in the stretching

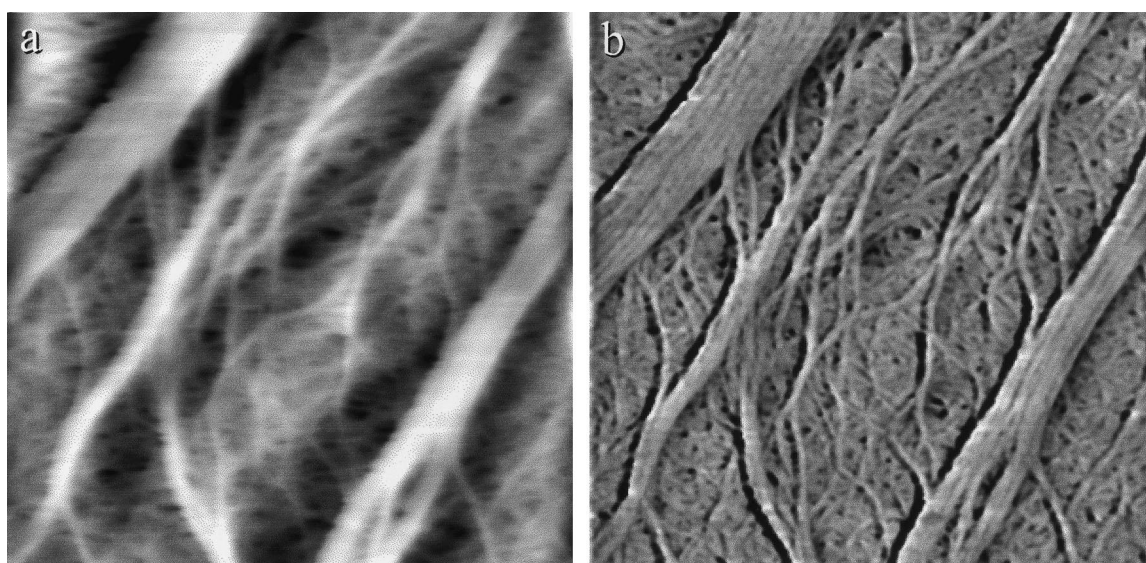


Fig. 4. Contact mode AFM topographic (a) and lateral force (b) images (scan area: $2.5 \times 2.5 \mu\text{m}^2$) obtained on part of the vein structure of BOPP-1 (MD and TD ratios are 5.2:1 and 9:1, respectively). The arrow in Fig. 1 shows the MD direction. Gray-scale ranges for the topographic and lateral force images are 41 nm and 1.6 nA, respectively. The unit of nA is for the photo-induced current in the photodetector which corresponds to the torsional movement of the cantilever.

direction because the stretching forces were being applied in that direction.

Fig. 3(a) and (b) shows representative non-contact mode AFM topographic images of areas $2.5 \mu\text{m}$ square obtained on the “normal” surface of the BOPP-1 film. It can be clearly seen, from Fig. 3(a) and (b), that the “normal” surface is characterized by a nanometer-scale fiber-like network structure. The apparent size of the fibers estimated from the AFM images is on the order of 40 nm. Fig. 3(a) shows that the fibers are aligned, mainly, parallel to the TD direction (or perpendicular to the MD direction). Because the TD stretching is performed after the MD stretching and its draw ratio (9:1) is much larger than that (5.2:1) of the MD stretching, the fiber orientation observed in Fig. 3(a) is therefore considered to arise mainly from the TD stretching. Fig. 3(b), on the other hand, shows that there is a network of fibers and that the thicker fibers are aligned nominally parallel to the MD direction even after TD stretching. From a number of measurements at different locations on the BOPP-1 film, we noted that the morphology shown in Fig. 3(a) dominates the “normal” surface, while the morphology shown in Fig. 3(b) is generally found near the larger vein structures.

We noticed from our AFM measurements that the fine fibers seen in Fig. 3 are sensitive to the cleanness (sharpness) of the tip. Sometimes when an old tip was used, the surface features (e.g., fibers) were found to be dilated. In most cases, this is found to be caused by contamination of the tip: when we cleaned such tips by exposing them to UV–ozone atmosphere, much better images were usually obtained once again. Therefore, the images shown in this paper were carefully obtained to ensure that the dilation effect from contamination of the tip was eliminated. It is obvious, on the other hand, that the BOPP film can act as a test sample to examine the performance of the tip.

The finer features of the large veins are seen much more clearly in Fig. 4, which shows the contact mode topographic (a) and lateral force (b) images obtained at a location on BOPP-1 where there was a concentration of the larger veins. The topographic image, although useful, reveals only the larger surface features. The lateral force image, however, shows a clear image of the veins on the BOPP-1 film surface. Fig. 4(b) shows that the direction of these veins is nominally parallel to the MD direction. The direction and thickness of the veins indicate that they are formed in the MD stretching and that the draw ratio is such that they remain basically intact after TD stretching. Of greater interest is the structure inherent in the larger veins. We can see clearly that the larger veins are made up of a number of narrower strands and that some single strands are pulling away from the bulk of the veins. The strands that are pulling away are thought to be caused by the TD stretching.

Because the lateral force image shown in Fig. 4(b) is useful for revealing topographic features of the veins, we will now briefly discuss the mechanism of lateral force imaging. When the tip encounters topographic features

during scanning, the interaction between the tip and the features results in a torsional movement of the cantilever, which defines the topographic features through the enhancement of their outlines. The basis for the enhancement of the contrast in the lateral force image is that, unlike the topographic image which provides height information, the lateral force image mainly reveals the abrupt changes in the topographic features. Lateral force microscopy seems to give clear details of the outlines of surface features at the cost of losing topographic height information.

The loading force applied to the surface during scanning in contact mode AFM is known to sometimes change the sample surface. For example, an applied force of 10 nN can change the morphology of crystallized polyethylene oxide films prepared on a mica surface [13]. Therefore, it is important to make sure that the film surface is not degraded while obtaining images such as those presented in Fig. 4. By imaging a larger area including the previously scanned area, we confirmed that the film surface was not degraded during scanning when a loading force of 1–5 nN was used to obtain the images. Therefore, the lateral force image presented in Fig. 4(b) shows a significant improvement in image resolution over topographic imaging without any accompanying surface degradation. In fact, we found that fibers on the BOPP film surface can be reoriented by mechanical scratching using large loading forces [14]. It should be noted that surface damage occurs when the imaging force in a contact mode AFM exceeds some certain threshold loading force [13].

The formation of the fiber-like network and veins, as seen in Figs. 3 and 4, arises from the arrangement of the polymer chains during mechanical stretching. Before stretching there should be no order to the polymer chains in the resin. We analyzed a uniaxially oriented (in the MD direction) PP film to examine the effect of the mechanical stretching. As shown in the topographic image presented in Fig. 2, stretching of the film in the MD direction causes the chains to align uniaxially in that direction. Those strands seen in Fig. 2 which are not transformed into smaller fibers during the subsequent TD stretching are thought to remain as the veins shown in Figs. 1 and 4. The strands seen in Fig. 2 undergo additional orientation when subjected to mechanical stretching in the TD direction, as shown in Figs. 3 and 4. From Fig. 4(b) it is easy to see that some of the strands at the surface are not as susceptible to the mechanical stretching in the TD direction and these strands remain on the surface as veins.

BOPP-1 was formed by stretching the film with a MD ratio of 5.2:1 followed by a TD ratio of 9:1. The much larger TD ratio is responsible for the predominance of fibers oriented in the TD direction as seen in Fig. 3(a). The veins which are observed in Figs. 1 and 4 are attributed to a number of strands at the surface which have been oriented in the MD direction after the MD stretching (e.g. see Fig. 2) but are resistant to the subsequent stretching in the TD direction. These observations lead us to believe that much

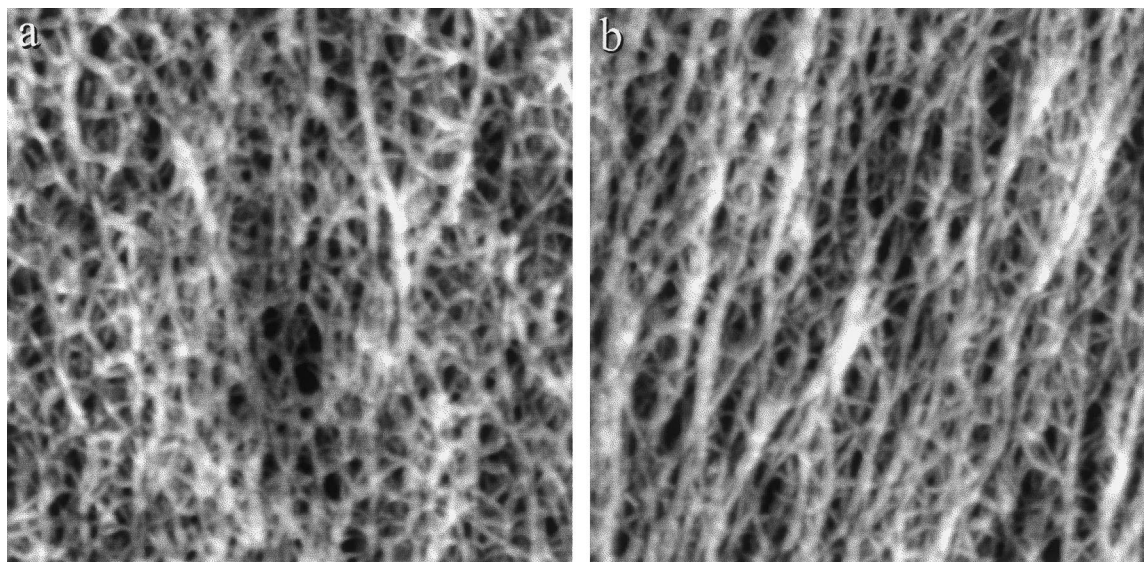


Fig. 5. Shown in (a) and (b) are two representative non-contact mode AFM topographic images (scan area: $2.5 \times 2.5 \mu\text{m}$) obtained on BOPP-2 (MD and TD ratios are 8:1 and 8.7:1, respectively). The MD direction is indicated by the arrow inserted in Fig. 1. Gray-scale ranges for the topographic images in (a) and (b) are 20 and 24 nm, respectively.

of the morphology of the PP can be related to the difference between the MD and TD ratios. Although only the surface morphology can be observed by AFM, we would think that the bulk microscopic structure of these films is basically similar to the surface structure seen in the AFM images. The veins seen on the surface are thought to be caused by local distribution of stretching force. This distribution of stretching force would have greater influence on the surface morphology than on the bulk microscopic structure. Therefore, we speculate that there are less veins in the bulk microscopic structure than on the surface.

We have confirmed that changes in the relationship between the MD and TD ratios affect the final morphology by analysing BOPP-2 which was fabricated with a MD ratio of 8:1 followed by a TD ratio of 8.7:1. The difference between the MD and TD ratios used for BOPP-2 is much smaller than that for BOPP-1. Two typical non-contact mode AFM topographic images of an area $2.5 \mu\text{m}$ square obtained at two different locations are shown in Fig. 5. It is clear that the surface is dominated by a fiber-like network structure in which the fibers are aligned similarly in the MD and TD directions as shown in Fig. 5(a). There are only a very few slightly thicker fibers oriented in the MD direction. Fig. 5(b) shows another image with more thicker fibers oriented in the MD direction. The apparent diameter of the smaller fibers is $\sim 40 \text{ nm}$ and the thicker fibers have a diameter of approximately twice of this size. In contrast to Fig. 3(a), the fibers seen in Fig. 5 do not show any dominating alignment in the TD direction. The similarity in the draw ratios for the BOPP-2 precluded the dominance of fibers in either the TD or MD directions, as shown in Fig. 5.

After imaging many locations using scan areas from 20 to $100 \mu\text{m}$, we noted that there were no veins on the surface of the BOPP-2 film (fabricated with a MD ratio of 8:1), while

there are many veins on the BOPP-1 film (fabricated with a MD ratio of 5.2:1). This difference in morphology could be partly explained as a result of the different draw ratios. It is presumed that the larger the MD ratio, the thinner the strands oriented in the MD direction. During the subsequent TD stretching process, the smaller strands should be more amenable to the TD stretching. As a result, few or no veins remained on the BOPP-2 film fabricated with a higher MD ratio.

There are other processing parameters which need to be considered, such as the draw temperatures and times as well as the quenching rates and temperatures. These parameters will also have an effect on the orientation of the fibers in BOPP films. Investigation of these effects on the fiber orientation will provide us with valuable insight into the relationship between the microstructure of the film and its physical properties.

4. Conclusions

Nanometer-scale fiber-like network structures on BOPP films were elucidated with AFM. We have clearly shown that the morphology of the film is determined by the relationship between the MD and TD ratios. The results reported here, which are summarized as follows, are useful in understanding the morphology of polymer films fabricated by mechanical stretching and show that one can control the film morphology by selecting appropriate MD and TD ratios.

1. A lower MD ratio (5.2:1) followed by a higher TD ratio (9:1) resulted in a morphology characterized by a network structure in which the small fibers showed a preferential arrangement in the TD direction. There

were thicker veins present in parts of the network which were nominally oriented in the MD direction.

2. For a higher MD ratio (8:1) accompanied by a similar TD ratio (8.7:1), the morphology was characterized by a network structure showing no predominant TD direction fiber alignment, and no larger veins oriented in the MD direction.

Acknowledgements

The authors are grateful to J.M. Strobel of 3M for providing some of the films used in this study.

References

- [1] Walzak MJ, Flynn S, Foerch R, Hill JM, Karbasheski E, Lin A, Strobel M. *Adhesion Sci Technol* 1995;9:1229.
- [2] Binnig G, Quate CF, Geber Ch. *Phys Rev Lett* 1986;56:930.
- [3] Nie H-Y, Walzak MJ, Berno B, McIntyre NS. *Appl Surf Sci* 1999;15:6484.
- [4] Aboulfaraj M, Ulrich B, Dahoun A, G'Sell C. *Polymer* 1993;34:4817.
- [5] Campbell RA, Phillips PJ, Lin JS. *Polymer* 1993;34:4809.
- [6] Stocker W, Schumacher M, Graff S, Lang J, Wittmann JC, Lovinger AJ, Lotz B. *Macromolecules* 1994;27:6948.
- [7] Snetivy D, Vancso GJ. *Polymer* 1994;35:461.
- [8] Tsukruk VV, Reneker DH. *Macromolecules* 1995;28:1370.
- [9] Castelein G, Coulon G, G'Sell C. *Polym Engng Sci* 1997;37:1694.
- [10] Hild S, Gutmannsbauer W, Luthi R, Fuhrmann J, Gruntherodt H-J. *J Polym Sci: Polym Phys* 1996;34:1953.
- [11] Overney RM, Luthi R, Haefke H, Frommer J, Meyer E, Gruntherodt H-J, Hild S, Fuhrmann J. *Appl Surf Sci* 1993;64:197.
- [12] Meyer G, Amer N. *Appl Phys Lett* 1990;57:2089.
- [13] Nie H-Y, Motomatsu M, Mizutani W, Tokumoto H. *J Vac Sci Technol B* 1997;15:1388.
- [14] Nie H-Y, Walzak MJ, Berno B, McIntyre NS. *Langmuir* 1999;144–145:627.